THE JOURNAL OF PHYSICAL CHEMISTRY Letters

Letter

pubs.acs.org/JPCL

Fabrication of PEDOT Nanocone Arrays with Electrochemically Modulated Broadband Antireflective Properties

Seulgi So, Han Wai Millie Fung, Kellen Kartub, Adam M. Maley, and Robert M. Corn*

Department of Chemistry, University of California-Irvine, Irvine, California 92697, United States

Supporting Information

ABSTRACT: Ordered nanocone arrays of the electroactive polymer poly(3,4-ethylenedioxythiophene) (PEDOT) were fabricated by the simultaneous oxygen plasma etching of an electrodeposited PEDOT thin film coated with a hexagonally closed packed polystyrene bead monolayer. PEDOT nanocone arrays with an intercone spacing of 200 nm and an average nanocone height of 350 nm exhibited a low broadband reflectivity of <1.5% from 550 to 800 nm. Electrochemical modulation of the oxidation state of the PEDOT nanocone array film was used to change both its ex situ absorption spectrum (electrochromism) and reflection spectrum (electroreflectivity). The sign of the PEDOT nanocone array electroreflectivity was opposite to that observed from unmodified PEDOT thin films; this significant difference is attributed to the unique optical behavior of nanostructured surfaces with an interfacial layer that contains a graded mix of air and highly absorptive nanocones. The combined electrochromic and electroreflective behavior of the antireflective PEDOT nanocone array films should find promising applications in solar energy cells, sensors and other optical devices.

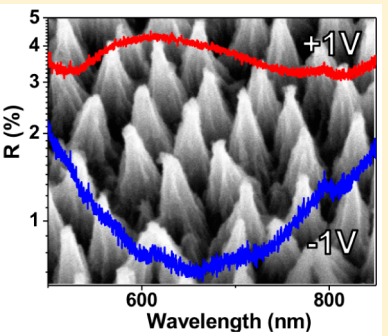

Periodic nanocone arrays are unique nanostructured surfaces with very useful antireflective and hydrophobic properties that have been incorporated into both natural systems, such as moths' eyes and lotus leaves,[1−3] and also modern technological devices, such as solar cells and self-cleaning windows.[4−6] Recently, we have developed a very simple method for fabricating polymeric 2D hexagonal nanocone arrays over large areas (cm^2) by the simultaneous oxygen plasma etching of a colloidal monolayer of polystyrene (PS) beads and an underlying polymer substrate. For the case of flexible fluorinated ethylene propylene (FEP) substrates, we fabricated FEP nanocone arrays and then coated them with a 50 nm gold thin film to create a plasmonic nanocone surface that was highly antireflective[7] and also exhibited tunable superhydrophobic properties.[8] We demonstrate here that our nanocone array fabrication strategy can be used to create nanocone arrays from thin films of the electroactive polymer poly(3,4-ethylenedioxythiophene) (PEDOT). Thin PEDOT films have been studied extensively for their transmissive electrochromic properties;[9−13] we show that PEDOT nanocone arrays formed by the oxygen plasma etching of an electrodeposited PEDOT thin film coated with a hexagonally closed packed (hcp) PS bead monolayer exhibit excellent broadband antireflectivity. Moreover, the oxidation state of the PEDOT nanocone array film can be modulated electrochemically and remains fixed when removed under potentiostatic control. Both the absorption spectrum and reflectivity spectrum are found to vary with film oxidation state, but each in a different manner due to different optical effects. Changes in the reflectivity spectrum of the PEDOT nanocone arrays with oxidation state were completely opposite to those observed from unmodified PEDOT thin films; this difference is attributed to the unique dependence of the PEDOT nanocone array reflectivity on the complex interfacial refractive index.

PEDOT nanocone arrays were fabricated from the simultaneous oxygen plasma etching of electrodeposited PEDOT thin films coated with an hcp PS bead monolayer. The formation of a PEDOT thin film through the electropolymerization and electrodeposition of "3,4-ethylenedioxythiophene" (EDOT) has been demonstrated previously for films up to 300 nm in thickness.[12,14−16] To create stable thick PEDOT films, we developed a slightly modified electrodeposition process in which a very thin PEDOT:PSS layer was first spin-coated onto a transparent fluorine tin oxide (FTO) conductive substrate prior to the EDOT electropolymerizaton. The thickness of the electrodeposited PEDOT thin films was controlled by the electrodeposition time and set to a value of 450 nm as measured by SEM. A PS bead monolayer was then deposited onto the PEDOT thin film by a spin-coating process in ethanolic solution. (Full details of our electrodeposition procedure, a plot of electrodeposition current versus time, SEM thickness measurement, and colloidal monolayer formation procedure are given in the Supporting Information (SI).). As shown in the scheme in Figure 1a, exposure of this surface to oxygen plasma etching created the PEDOT nanocone array. The PS bead monolayer initially protects the PEDOT thin film, but as the plasma etching constantly reduces the bead size, the amount of protected surface constantly decreases as the nanocone array is formed. The spacing of the nanocones

Received: December 7, 2016
Accepted: January 12, 2017
Published: January 12, 2017

DOI: 10.1021/acs.jpclett.6b02873
J. Phys. Chem. Lett. 2017, 8, 576−579

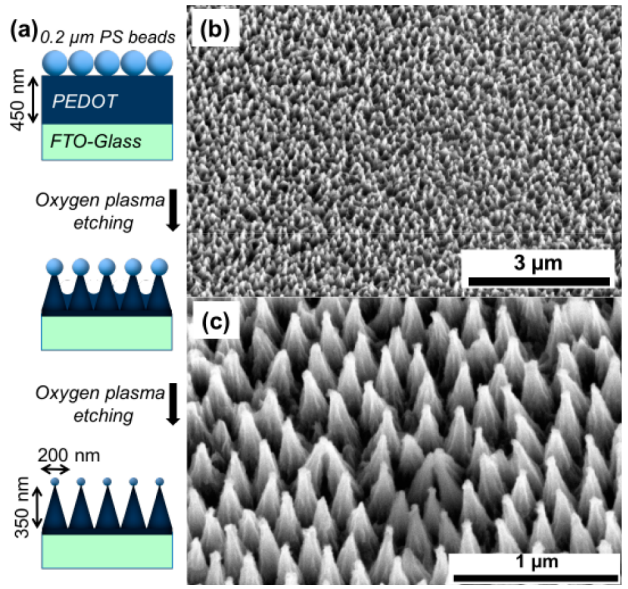

Figure 1. (a) Schematic diagram for the fabrication of PEDOT nanocone arrays (height: 350 nm, spacing: 200 nm) by oxygen plasma etching of a 450 nm electrodeposited PEDOT film on FTO-glass coated with a 200 nm hcp PS bead monolayer. (b) SEM image of PEDOT nanocone arrays with low magnification and (c) detailed SEM image of PEDOT nanocones with high magnification and a tilted view.

within the array is controlled by the original PS bead diameter, and the height of the nanocones is controlled by both the size of the PS beads and the thickness of the electrodeposited PEDOT thin film as well as the differential bead/film etching rate. Two SEM images of a typical PEDOT nanocone array surface are shown in Figure 1b,c. The nanocones in this array were formed by 90 s of oxygen plasma etching of a 450 nm PEDOT thin film coated with an hcp monolayer of 200 nm diameter PS beads. The resultant nanocone array had an average height of 350 nm, and a small amount of residual PS can be seen on the nanocones in Figure 1c. To ensure removal of this residual PS, the films were thoroughly rinsed with tetrahydrofuran after etching.

The PEDOT nanocone array surfaces created by this plasma etching process exhibited a very low reflectivity over a wide wavelength range. The reflectivity spectrum of the PEDOT nanocone array at an incident angle of 8° is shown in Figure 2 (blue spectrum). Similar reflectivity spectra were observed at higher incident angles (reflectivity spectra obtained at incident angles of 45 and 67.5° are shown in Figure S4 of the SI.). The PEDOT nanocone array reflectivity is relatively featureless and <1.5% R over the entire wavelength range of 550 to 800 nm. For comparison, the reflectivity spectrum of an unmodified 450 nm electrodeposited PEDOT film (black spectrum) is shown in Figure 2 (a similar spectrum for an unmodified 350 nm electrodeposited PEDOT film is shown in SI). The PEDOT nanocone array surface had lower percent reflectivity values at all wavelengths throughout the visible and near-infrared for both incident angles as compared with the unmodified PEDOT thin-film spectrum and most noticeably did not show the strong reflectivity increase feature at 570 nm that was observed for the unmodified film. Additionally, a plasmonic gold-coated FEP nanocone array (red spectrum)[7] is also shown in the Figure. We deduce that the mechanism for the broadband antireflectivity of the PEDOT nanocones is the same as in the case of

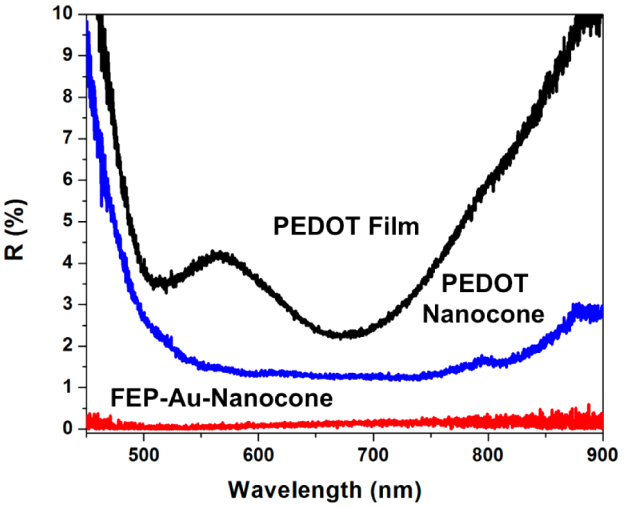

Figure 2. Reflectivity spectra at an incidence angle of 8° for a PEDOT nanocone array film (blue spectrum), an unmodified PEDOT thin film (black spectrum), and a plasmonic gold nanocone array thin film (red spectrum). The FEP-Au-nanocone array film was fabricated as described in ref 7.

the plasmonic gold nanocone arrays, although, as can be seen in the Figure, the PEDOT nanocone arrays are not as antireflective as the gold-coated FEP nanocones. Silicon nanocone array surfaces previously described by other authors also show similar broadband antireflection properties.[17−19] The reflectivity of nanocone array surfaces has been previously modeled as a combination of graded refractive index and enhanced thin-film absorption.[17,20,21] The higher aspect ratio of the gold-coated FEP nanocone arrays and their better absorptive properties are the two reasons why the antireflectivity is better for those surfaces.[7]

Like all other previous studies of electrodeposited PEDOT thin films, the PEDOT nanocone array films were found to exhibit a reversible electrochromism due to the modulation of the PEDOT film oxidation state with electrode potential in a $LiClO_4$ solution.[12,22] In addition to observing the in situ PEDOT electrochromic behavior in an electrochemical cell, the PEDOT films could be removed from solution under potentiostatic control to examine both their absorption spectrum and antireflective properties in air. Figure 3 plots the absorption spectra of the PEDOT nanocone arrays after the removal from solution at three different potentials: + 1.0, 0.0, and −1.0 V versus Ag/AgCl (all potentials were held for 20s before removal from solution). As shown previously by other researchers, the electrochromic behavior of PEDOT arises from changes in the electrochemical doping of the thin film, with the more reduced state (−1.0 V) being highly colored and the more oxidized state (+1.0 V) being less absorptive.[9,13,16] This can be seen both in the ex situ absorption spectra as well as in the two photographs of the PEDOT nanocone array film at +1.0 and −1.0 V that are also shown in the Figure. These spectra are qualitatively similar to spectra obtained from an unmodified PEDOT thin film removed at the same potentials (see Figure S5 in the SI).

In contrast, the variations in the ex situ reflectivity spectra for PEDOT nanocone arrays removed at different electrode potentials were surprisingly different as compared with unmodified PEDOT thin film surfaces. Figure 4a,b shows reflectivity spectra from a PEDOT nanocone array and an

DOI: 10.1021/acs.jpclett.6b02873
J. Phys. Chem. Lett. 2017, 8, 576−579

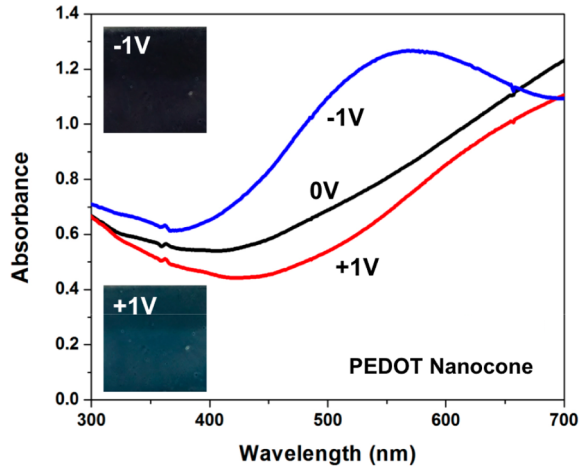

Figure 3. Electrochromic behavior of PEDOT nanocone arrays. UV–visible absorption spectra of PEDOT nanocone arrays removed from solution after 20 s under potentiostatic control at three potentials: −1.0 (blue spectrum), 0.0 (black spectrum), and +1.0 V (red spectrum) versus Ag/AgCl. The two inserted photographs show the different colors of the PEDOT nanocone array sample at −1.0 (dark-purple/black) and +1.0 V (blue).

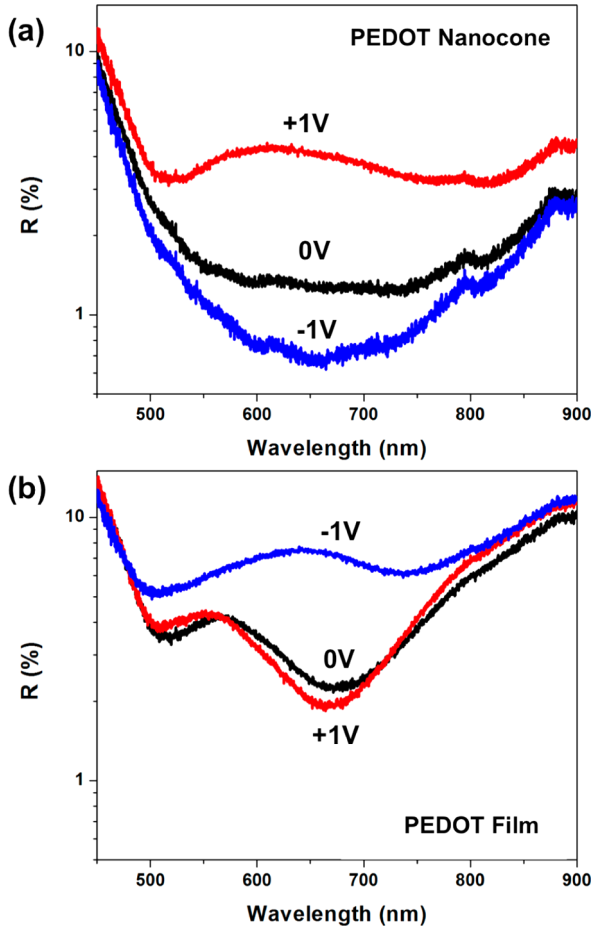

Figure 4. Electrochemically modulated reflectivity spectra for (a) PEDOT nanocone arrays and (b) unmodified PEDOT thin films that were removed from solution after 20s at three different applied potentials: −1.0 (blue spectrum), 0.0 (black spectrum), and +1.0 V (red spectrum). The angle of incidence for the reflectivity spectra was 8°.

unmodified PEDOT thin film, respectively, after being removed from solution at the same three applied potentials as in Figure 3 (−1.0, 0.0, and +1.0 V). The most dramatic differences are between spectra taken at −1.0 to +1.0 V, where the reflectivity has significantly *increased* at all wavelengths for the PEDOT nanocone array film but has *decreased* for the unmodified PEDOT thin film. The largest effect occurs at ∼650 nm, where the PEDOT nanocone array reflectivity increases 5-fold (from 0.67% *R* up to 4.14% *R*), whereas the unmodified PEDOT thin film reflectivity decreases 4-fold (from 7.6% *R* down to 2.0% *R*). The featureless reflectivity spectrum of the PEDOT nanocone array in Figure 4a does not change significantly at the three different applied potentials, whereas there are significant band shifts in the spectrum of the unmodified PEDOT thin film in Figure 4b. Additionally, when comparing changes in the reflectivity spectra from films removed at 0.0 and +1.0 V, a proportional increase in the reflectivity spectrum was observed for the PEDOT nanocone array, whereas only relatively small reflectivity changes were observed for the unmodified PEDOT thin film. It is clear from the spectra in Figure 4 that the optical mechanism for the broadband electroreflectivity observed from the PEDOT nanocone array film must be very different from the mechanism for the electroreflectivity observed from the unmodified PEDOT film. To try to understand this effect, we performed three-phase Fresnel reflectivity calculations (air/film/substrate, *n*1/*n*2/*n*3 as described in Figure S6 in the SI) to show that an increase in film absorption (as modeled by an increase in the imaginary component of the film RI, *n*2 = 1.5 + *xi*, where *x* goes from 0 to 0.5) leads to a higher specular reflectivity at all angles. This is what we observed for the unmodified PEDOT films. In contrast, the PEDOT nanocone films showed the opposite behavior: An increase in nanocone absorptivity actually resulted in a decrease in the specular reflectivity. This effect has been previously observed for both the gold plasmonic nanocone arrays[7] and silicon nanocone array surfaces.[17−19] The presence of highly absorbing nanocones on the surface results in a combination of multiple internal reflection, absorption, and scattering processes that lead to a reduced reflectivity at all incident angles.

In summary, we have demonstrated that the fabrication process used previously to create gold plasmonic nanocone arrays also can be used with thin films of the electroactive polymer PEDOT to create electroreflective nanocone arrays over large areas. The PEDOT nanocone array surfaces exhibited a good broadband antireflectivity throughout the visible and near-infrared wavelength regions due to the graded interfacial complex refractive index created by the PEDOT nanocones. Additionally, the broadband antireflectivity of the nanocone array surface could be controlled by the electrochemical modulation of the oxidation state of the PEDOT nanocones. The changes observed in the ex situ reflectivity spectra of the PEDOT nanocone arrays with oxidation state were opposite to those observed from unmodified PEDOT thin films; we attribute this marked difference to the unique optical behavior (a combination of broadband reflection, scattering, and absorption) of the air−nanocone array interface for the case where the nanocone complex refractive index has a significant imaginary component. In this Letter, the electroreflectivity of the PEDOT nanocone arrays was probed with ex situ spectra; in future work we will further characterize the reversible in situ electroreflective behavior with real-time reflectivity measurements. The antireflective and electrochromic PEDOT semiconductor nanocone array films

DOI: 10.1021/acs.jpclett.6b02873
J. Phys. Chem. Lett. 2017, 8, 576−579

described here should find applications in solar energy cells, optical sensors, and optical devices.

■ ASSOCIATED CONTENT

Supporting Information

The Supporting Information is available free of charge on the ACS Publications website at DOI: 10.1021/acs.jpclett.6b02873.

Experimental details of PEDOT nanocone array fabrication and characterization, electrochemical data of PEDOT electropolymerization and electrodeposition, 45 and 67.5° incident angle PEDOT nanocone array and unmodified PEDOT thin-film reflectivity spectra, SEM images, and UV−vis absorption spectra of unmodified PEDOT thin films. (PDF)

■ AUTHOR INFORMATION

Corresponding Author

*E-mail: rcorn@uci.edu.

ORCID

Adam M. Maley: 0000-0003-1851-984X

Robert M. Corn: 0000-0002-4756-2161

Notes

The authors declare no competing financial interest.

■ ACKNOWLEDGMENTS

This work was supported by the National Science Foundation through grant CHE-1403506.

■ REFERENCES

(1) Celia, E.; Darmanin, T.; Taffin de Givenchy, E.; Amigoni, S.; Guittard, F. Recent Advances in Designing Superhydrophobic Surfaces. *J. Colloid Interface Sci.* **2013**, *402*, 1−18.

(2) Raut, H. K.; Ganesh, V. A.; Nair, A. S.; Ramakrishna, S. Anti-Reflective Coatings: A Critical, in-Depth Review. *Energy Environ. Sci.* **2011**, *4*, 3779−3804.

(3) Clapham, P. B.; Hutley, M. C. Reduction of Lens Reflexion by the "Moth Eye" Principle. *Nature* **1973**, *244*, 281−282.

(4) Tsui, K.; Lin, Q.; Chou, H.; Zhang, Q.; Fu, H.; Qi, P.; Fan, Z. Low-Cost, Flexible, and Self-Cleaning 3D Nanocone Anti-Reflection Films for High-Efficiency Photovoltaics. *Adv. Mater.* **2014**, *26*, 2805−2811.

(5) Leem, J. W.; Kim, S.; Lee, S. H.; Rogers, J. A.; Kim, E.; Yu, J. S. Efficiency Enhancement of Organic Solar Cells Using Hydrophobic Antireflective Inverted Moth-Eye Nanopatterned PDMS Films. *Adv. Energy Mater.* **2014**, *4*, 1301315.

(6) Wang, Y.; Lu, N.; Xu, H.; Shi, G.; Xu, M.; Lin, X.; Li, H.; Wang, W.; Qi, D.; Lu, Y.; Chi, L. Biomimetic Corrugated Silicon Nanocone Arrays for Self-Cleaning Antireflection Coatings. *Nano Res.* **2010**, *3*, 520−527.

(7) Toma, M.; Loget, G.; Corn, R. M. Fabrication of Broadband Antireflective Plasmonic Gold Nanocone Arrays on Flexible Polymer Films. *Nano Lett.* **2013**, *13*, 6164−6169.

(8) Toma, M.; Loget, G.; Corn, R. M. Flexible Teflon Nanocone Array Surfaces with Tunable Superhydrophobicity for Self-Cleaning and Aqueous Droplet Patterning. *ACS Appl. Mater. Interfaces* **2014**, *6*, 11110−11117.

(9) *PEDOT: Principles and Applications of an Intrinsically Conductive Polymer*; Kirchmeyer, S., Elschner, A., Reuter, K., Lovenich, W., Merker, U., Eds.; CRC Press, 2010.

(10) Sankaran, B.; Reynolds, J. R. High-Contrast Electrochromic Polymers from Alkyl-Derivatized Poly(3,4-Ethylenedioxythiophenes). *Macromolecules* **1997**, *30*, 2582−2588.

(11) Mortimer, R. J. Organic Electrochromic Materials. *Electrochim. Acta* **1999**, *44*, 2971−2981.

(12) Kumar, A.; Welsh, D. M.; Morvant, M. C.; Piroux, F.; Abboud, K. a.; Reynolds, J. R. Conducting Poly(3,4-Alkylenedioxythiophene) Derivatives as Fast Electrochromics with High-Contrast Ratios. *Chem. Mater.* **1998**, *10*, 896−902.

(13) Ruffo, R.; Celik-Cochet, A.; Posset, U.; Mari, C. M.; Schottner, G. Mechanistic Study of the Redox Process of an in Situ Oxidatively Polymerised poly(3,4-Ethylene-Dioxythiophene) Film. *Sol. Energy Mater. Sol. Cells* **2008**, *92*, 140−145.

(14) Randriamahazaka, H.; Sini, G.; Tran Van, F. Electrodeposition Mechanisms and Electrochemical Behavior of Poly (3, 4-Ethylenedithiathiophene). *J. Phys. Chem. C* **2007**, *111*, 4553−4560.

(15) Nguyen, V. Q.; Schaming, D.; Martin, P.; Lacroix, J. C. Highly Resolved Nanostructured PEDOT on Large Areas by Nanosphere Lithography and Electrodeposition. *ACS Appl. Mater. Interfaces* **2015**, *7* (39), 21673−21681.

(16) Deutschmann, T.; Oesterschulze, E. Micro-Structured Electrochromic Device Based on poly(3,4-Ethylenedioxythiophene). *J. Micromech. Microeng.* **2013**, *23* (6), 065032.

(17) Zhu, J.; Yu, Z.; Burkhard, G. F.; Hsu, C.-M.; Connor, S. T.; Xu, Y.; Wang, Q.; McGehee, M.; Fan, S.; Cui, Y. Optical Absorption Enhancement in Amorphous Silicon Nanowire and Nanocone Arrays. *Nano Lett.* **2009**, *9* (1), 279−282.

(18) Wang, K. X.; Yu, Z.; Liu, V.; Cui, Y.; Fan, S. Absorption Enhancement in Ultrathin Crystalline Silicon Solar Cells with Antireflection and Light-Trapping Nanocone Gratings. *Nano Lett.* **2012**, *12* (3), 1616−1619.

(19) Jeong, S.; Garnett, E. C.; Wang, S.; Yu, Z.; Fan, S.; Brongersma, M. L.; McGehee, M. D.; Cui, Y. Hybrid Silicon Nanocone-Polymer Solar Cells. *Nano Lett.* **2012**, *12* (6), 2971−2976.

(20) Brongersma, M. L.; Cui, Y.; Fan, S. Light Management for Photovoltaics Using High-Index Nanostructures. *Nat. Mater.* **2014**, *13* (5), 451−460.

(21) Wang, Z. Y.; Zhang, R. J.; Wang, S. Y.; Lu, M.; Chen, X.; Zheng, Y. X.; Chen, L. Y.; Ye, Z.; Wang, C. Z.; Ho, K. M. Broadband Optical Absorption by Tunable Mie Resonances in Silicon Nanocone Arrays. *Sci. Rep.* **2015**, *5*, 7810.

(22) Aubert, P. H.; Argun, A. A.; Cirpan, A.; Tanner, D. B.; Reynolds, J. R. Microporous Patterned Electrodes for Color-Matched Electrochromic Polymer Displays. *Chem. Mater.* **2004**, *16* (12), 2386−2393.

DOI: 10.1021/acs.jpclett.6b02873
J. Phys. Chem. Lett. 2017, 8, 576−579